



The synthesis and thermal stability of $\text{CaKCe}(\text{PO}_4)_2$ phosphate. Phase equilibria in the CaKPO_4 – CePO_4 system

Aleksandra Matraszek*, Irena Szczygieł, Teresa Znamierowska

Department of Inorganic Chemistry, Faculty of Engineering and Economics, Wrocław University of Economics, Komandorska 118/120, 53-345 Wrocław, Poland

ARTICLE INFO

Article history:

Received 19 October 2012

Received in revised form 6 December 2012

Accepted 10 December 2012

Available online 20 December 2012

Keywords:

Rare earth alloys and compounds

Phase diagrams

Thermal analysis

Chemical synthesis

X-ray diffraction

ABSTRACT

The compound $\text{CaKCe}(\text{PO}_4)_2$ was obtained using respectively the ceramic method, the Pechini method and the hydrothermal method. The low-temperature (Pechini and hydrothermal) methods yielded homogenous powders with a crystallite size up to 24 nm.

The compound has a hexagonal structure with parameters of an elementary cell: $a = b = 7.0468(8)$ Å and $c = 6.4367(0)$ Å. The $\text{CaKCe}(\text{PO}_4)_2$ phosphate occurs in one polymorphic form.

A phase equilibrium diagram of the CaKPO_4 – CePO_4 system has been established on the basis of XRD, DTA/DSC/TGA results. The initial phosphates were found to form one intermediate compound, $\text{CaKCe}(\text{PO}_4)_2$, with molar ratio $\text{CaKPO}_4:\text{CePO}_4 = 1:1$, melting incongruently at a temperature of 1530 °C according to the reaction: $\text{CaKCe}(\text{PO}_4)_{2(\text{cr})} \rightarrow \text{CePO}_{4(\text{cr})} + \text{L}$. At a temperature of 1440 °C an eutectic was found to be present in the CaKPO_4 – CePO_4 system at $x(\text{CePO}_4) = 0.25$.

© 2012 Published by Elsevier B.V.

1. Introduction

The research data published in recent decades indicate a high application potential of multicomponent phosphates with the formula $\text{CaKLn}(\text{PO}_4)_2$, where Ln – a rare-earth element [1–10]. The compounds have a hexagonal structure with unit-cell parameters $a = b \approx 7.0$ and $c \approx 6.4$ Å [11,12]. The structure is like that of rhabdophanes, i.e. compounds of the $\text{LnPO}_4 \cdot n\text{H}_2\text{O}$ type. It is characterized by the presence of longitudinal spaces formed by $(\text{Ln}, \text{Ca})\text{-PO}_4\text{-}(\text{Ln}, \text{Ca})$ chains running parallel to axis c . Potassium atoms are placed in the spaces [12]. This crystal structure suggests that compounds of this kind may be good ionic conductors. The $\text{CaKLn}(\text{PO}_4)_2$ compounds, where $\text{Ln} = \text{La}, \text{Eu}$ and Y , crystallizing in the monoclinic system (the monazite structure), were obtained through precipitation from aqueous salt solutions [11,13] too.

In [3,14], experimental difficulties in obtaining pure $\text{CaKLn}(\text{PO}_4)_2$ phases through synthesis in solid state were encountered. In the same papers it was suggested that the thermal stability of the preparations is limited.

Compounds of the formula $\text{CaKLn}(\text{PO}_4)_2$ form in CaKPO_4 – LnPO_4 binary systems. In [11] a phase diagram of the system for $\text{Ln} = \text{La}$ was presented. It was found that this phosphate undergoes polymorphic transition at 1120 °C. At this temperature the structure changes from low-temperature-monoclinic (β) to hexagonal (α). According to the results [11], at a temperature of 1480 °C the ternary phosphate undergoes peritectic decomposition.

* Corresponding author. Tel.: +48 71 368 0321; fax: +48 71 368 0292.

E-mail address: aleksandra.matraszek@ue.wroc.pl (A. Matraszek).

Phosphate CaKPO_4 occurs in two structural forms and melts at 1560 °C. The low-temperature form has an orthorhombic structure, whereas the high-temperature form has a hexagonal structure [15]. The polymorphic change of this phosphate is quite complicated and takes place in a temperature range of 600–660 °C [16].

Cerium orthophosphate has one thermodynamically stable polymorphic form (monazite) with a monoclinic structure [17,18], melting congruently at a temperature of 2072 °C [19].

The aim of the present research was to characterize the thermal behavior of $\text{CaKCe}(\text{PO}_4)_2$, i.e. to determine its thermal stability and melting temperature and to verify the previously mentioned reports about the existence of additional polymorphic forms. Moreover, in order to solve the problems with obtaining pure compounds, alternative synthesis routes of $\text{CaKCe}(\text{PO}_4)_2$ have been proposed. The compound $\text{CaKCe}(\text{PO}_4)_2$ was for the first time obtained using hydrothermal and modified Pechini methods. The hydrothermal syntheses consist in heating solutions under elevated pressure, which leads to precipitation of deposits. As a result, it is possible to obtain morphologically uniform and unagglomerated crystallites whose size is a function of temperature and/or synthesis time [20]. The Pechini method is a kind of sol–gel techniques [21]. It ensures good control of the stoichiometry of multicomponent compounds and a considerable reduction in phase sintering temperature (to below 600 °C). Our team has successfully used this method to obtain other phosphates [22,23].

Another aim of this research was to determine the phase relations in the CaKPO_4 – CePO_4 system, with a particular regard for the possible formation of limited solid solutions between the initial orthophosphates and the intermediate $\text{CaKCe}(\text{PO}_4)_2$ compound.

The existence of phases with a variable composition has been several times reported in papers dealing with phosphates systems with $LnPO_4$ [24–27]. The existence of such solid solutions based on rhabdophane would enable modification of physicochemical properties of the compound to a large extent.

2. Experimental

The $CaKPO_4$ and $CaKCe(PO_4)_2$ compounds for the phase equilibria study were prepared in a solid state by a ceramic method. The following analytical reagents were used to obtain the compounds: $CaCO_3$, $CaHPO_4$, K_2CO_3 , $Ce(NO_3)_3 \cdot 6H_2O$ and H_3PO_4 (85%) (analytical grade, POCh Gliwice). The $CePO_4$ was obtained by precipitation from a dilute aqueous solution of H_3PO_4 . The molar ratio of $H_3PO_4 : Ce(NO_3)_3 \cdot 6H_2O : H_2O$ was 1:0.023:25. The acidic solution of cerium nitrate was boiled under reflux for at least 6 h. The obtained precipitate was filtered and washed several times with hot distilled water. Finally, the powder was calcined at 1400 °C for 2 h to expel moisture and adsorbed pyrophosphates.

The $CaKPO_4$ compound was synthesized according to the synthesis route proposed in [16] from a stoichiometric amounts of K_2CO_3 and $Ca_2P_2O_7$, which were carefully ground in a vibratory mill (Fritsch, Pulverisette 23) in a presence of acetone. The powder was calcined 10 h at 1000 °C, ground again with acetone in the vibratory mill, pelletized and sintered 1 h at 1300 °C.

The $CaKCe(PO_4)_2$ phosphate was obtained by a ceramic method from stoichiometric mixture of $CePO_4$ and $CaKPO_4$ in a similar route as $CaKPO_4$ with following sintering parameters: 1000 °C/10 h and 1050 °C/10 h.

The samples of the $CaKPO_4$ – $CePO_4$ system with the composition $((1-x)CaKPO_4 + (x)CePO_4)$, where $x(CePO_4) < 0.50$, were synthesized from $CaKCePO_4$ and $CaKPO_4$. The samples with higher $CePO_4$ concentration were obtained from $CaKCe(PO_4)_2$ and $CePO_4$ compounds. The initial mixtures were ground in acetone, pelletized, and sintered 10 h at 1000 and 10 h at 1080 °C. All samples were ground in vibratory mill between the consecutive heating steps.

The $CaKCe(PO_4)_2$ compound was also obtained by a modified Pechini route and by a hydrothermal method. In the Pechini process following nitrates were used in stoichiometric ratios: $Ce(NO_3)_3 \cdot 6H_2O$, $Ca(NO_3)_2 \cdot 4H_2O$ and KNO_3 . The salts were dissolved in a small amount of distilled water. Citric acid (CA) and ethylene glycol (EG) were added to the solution in the CA:EG:Ce molar ratio of 4:8:1. The obtained solution has been heated at 80 °C under mixing until a viscous liquid obtained. Then $NH_4H_2PO_4$ in the appropriate molar ratio was added under stirring. The heating has been continued until a foam obtained, then the sample was put in an electric drier for 20 h at 120 °C. Calcination of dried gel was carried out in a furnace preheated at 500 °C for 10 h.

The $CaKCe(PO_4)_2$ powder was also obtained under short-lasting hydrothermal conditions. The chemical reagents, Ce(III) nitrate hexahydrate, calcium nitrate tetrahydrate and $K_3PO_4 \cdot 7H_2O$ were used in the 1:1:22 M ratio with the concentration of cerium of 0.04 mol/dm³. The nitrates were diluted with water, then potassium phosphate was added and the solution was diluted to obtain 50 ml of milky sol. As obtained sol was used for hydrothermal process. The hydrothermal reactions were performed in a Magnum II autoclave (Ertec, Poland) with heating of the samples by microwaves of the maximal power of 600 W. The syntheses were controlled by temperature measurement performed at the bottom part of Teflon reactor. The synthesis was carried out for 1 h at a maximal temperature of 240 °C. As obtained fine precipitates were centrifuged, washed several times with distilled water and dried at 120 °C.

Phase analysis of obtained powders was made using XRD technique and a Siemens D5000 diffractometer equipped with a copper radiation tube. The measurements were performed in 2θ angle range of 10–60° with a 0.02° step and at least 2 s per step. Silicon (99.995% ABCR GmbH) was used as an internal standard for refinement of structure parameters. Lattice constants of the $CaKCe(PO_4)_2$ unit cell were refined using Checkcell software [28].

The surface area value of $CaKCe(PO_4)_2$ samples obtained by various methods were determined by multipoint BET method by nitrogen adsorption using Autosorb 1, Quantachrome Autosorb Automated Gas Sorption System (Quantachrome Instruments). The mean grain size of powders was estimated using the relation: $d_{BET} = \frac{6}{S_{BET} \rho_{th}}$, where S_{BET} is the measured specific surface area of powders and ρ_{th} equal 3.65 g cm⁻³ is the theoretical density of the $CaKCe(PO_4)_2$.

The DTA/TGA experiments were carried out using Derivatograph 3427 (MOM, Hungary). Samples were heated in a temperature range of 20–1400 °C (heating rate: 7.5 °C min⁻¹, Pt crucible, sample mass 450–600 mg, air atmosphere). The SET-SYS™ apparatus (TG-DSC 1500; Setaram) was used for DSC/TGA studies. From 15 to 40 mg of the powdered samples were placed in a Pt crucible and heated to 1400 °C at a heating rate of 10 °C min⁻¹ using Ar as the purge gas. The temperature and sensitivity calibration factor for the thermal experiments were obtained at melting points of NaCl (801 °C), $Ca_2P_2O_7$ (1353 °C) and K_2SO_4 (1070 °C) and for the phase transition temperature of the latter compound (583 °C).

The temperatures above 1400 °C were determined by observing the behavior of pelletized powders by means of an optical pyrometer (Cyclops 100, Ametek Land) calibrated against melting points of SiO_2 (5N, Carl Roth GmbH), Na_3PO_4 and Ca_3

$(PO_4)_2$. The experiments were performed under Ar atmosphere in a horizontal tubular furnace with molybdenum heating wires. Phase composition of molten and cooled to room temperature samples was controlled by XRD method.

3. Results and discussion

3.1. Synthesis and characterization of $CaKCe(PO_4)_2$ compound

The $CaKCe(PO_4)_2$ compound was obtained using respectively the solid state synthesis (ceramic technique), the hydrothermal and the Pechini methods. The phase purity of the obtained powders was evaluated by XRD, DTA/DSC/TGA and FTIR techniques.

Fig. 1 shows the X-ray diffraction patterns of the compound obtained by the methods mentioned above. An analysis of the diffractograms revealed presence of a phase with a rhabdophane structure. The indexed pattern of the $CaKCe(PO_4)_2$ obtained by the ceramic method confirmed the presence of a compound with a hexagonal structure and unit-cell parameters $a = b = 7.0468(8)$ Å and $c = 6.4367(0)$ Å. The parameters are slightly higher than the ones given for the $CaKCe(PO_4)_2$ compound [12], due to smaller ionic radius of Nd^{3+} than that of Ce^{3+} [29]. Consequently, the unit cell volume of $CaKCe(PO_4)_2$ should also be larger than that of neodymium phosphate $CaKCe(PO_4)_2$.

Since the X-ray pattern of the $CaKCe(PO_4)_2$ is similar to the spectrum of $CePO_4 \cdot nH_2O$, the obtained powders were additionally characterized by means of Fourier-transform infra-red spectroscopy (FTIR). The FTIR spectra of the powders synthesized by the different methods are shown in Fig. 2. For comparison, spectrum of $CePO_4 \cdot nH_2O$ (rhabdophane) was included. The presented spectra of $CaKCe(PO_4)_2$ (curves B–D in Fig. 2) and rhabdophane (Fig. 2 curve A) differ in the ranges of 1200–850 and 650–400 cm⁻¹, i.e. in the ranges in which main vibrations of PO_4 groups are observed. The difference in the symmetry of the PO_4 groups in the $CaKCe(PO_4)_2$ and $CePO_4 \cdot nH_2O$ phosphates is indicated by:

- The presence of two absorption bands at a frequency of 600 cm⁻¹ for $CaKCe(PO_4)_2$, instead of one band for $CePO_4 \cdot nH_2O$.
- The appearance of additional absorption bands for $CaKCe(PO_4)_2$ in wave numbers range of 500–400 cm⁻¹.
- The presence of an intensive absorption band at about 950 cm⁻¹.

The change in the symmetry of the PO_4 from D_2 (in rhabdophane) to C_2 (in ternary phosphate) was described in detail in

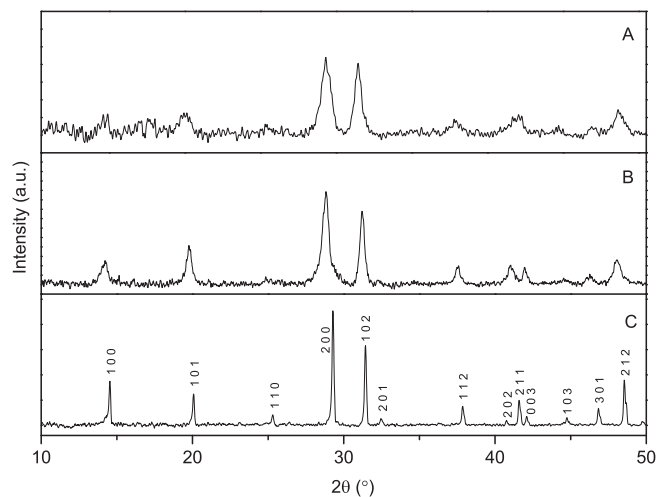


Fig. 1. The XRD patterns of $CaKCe(PO_4)_2$ compound obtained by hydrothermal process dried at 120 °C (A), by Pechini method sintered 10 h at 500 °C (B), and synthesized in solid state at 1050 °C (C).

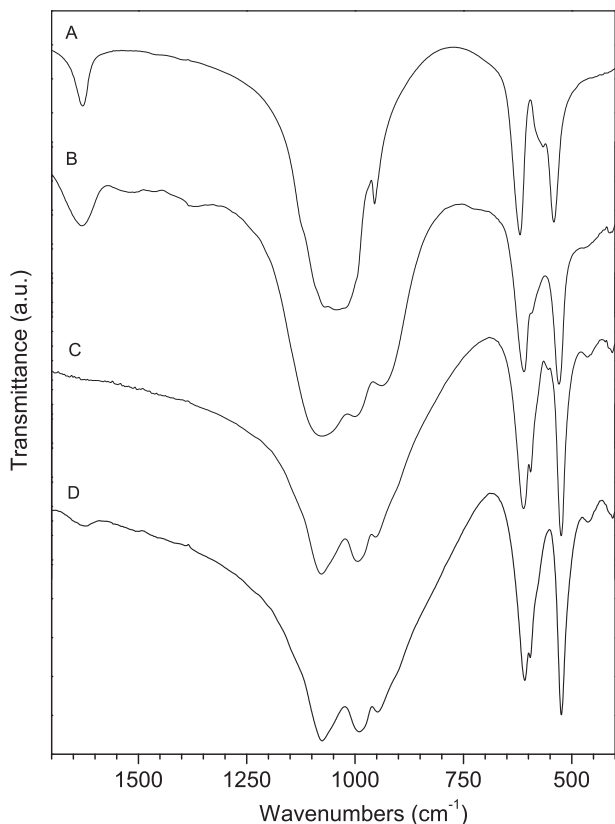


Fig. 2. The FTIR spectra of $\text{CePO}_4 \cdot n\text{H}_2\text{O}$ (rhabdophane) (A) and $\text{CaKCe}(\text{PO}_4)_2$ obtained by hydrothermal process and dried at 120 °C (B), sintered 2 h at 1000 °C (C) as well as synthesized by Pechini method after sintering at 1000 °C for 10 h (D).

[30] and was correlated to different ionic environment of the PO_4 groups in compounds $\text{CePO}_4 \cdot n\text{H}_2\text{O}$ and $\text{CaKCe}(\text{PO}_4)_2$.

In addition, strong bands at about 1630 cm^{-1} are visible in the spectrum of the $\text{CaKCe}(\text{PO}_4)_2$ compound obtained by the hydrothermal route and in the spectrum of the $\text{CePO}_4 \cdot n\text{H}_2\text{O}$ phosphate (the curves B and A in the Fig. 2, respectively). The bands are characteristic of the bending vibrations of water molecules. The presence of the bands in the spectra could be attributed to the presence of zeolitic water molecules in the rhabdophane structure and to the humidity in the ternary phosphate.

Moreover, the X-ray patterns of the samples obtained by the low-temperature (Pechini and hydrothermal) methods were characterized by a considerable broadening of reflections (curves A and B in Fig. 1). This is due to the smaller crystallite size of the ternary phosphate. In order to estimate the average size of the crystallites in the prepared samples the Scherrer equation was used: $D = \frac{K\lambda}{B \cos \theta}$, where D/nm is the average crystallite size in the direction perpendicular to the (hkl) plane of a given reflection. $K = 0.9$ is the Scherrer constant [31], $\lambda = 0.154 \text{ nm}$ – the wavelength of radiation $\text{CuK}\alpha$ and B – the corrected full-width at the half-maximum (FWHM) of the diffraction peak at angle θ . The calculated average sizes of the crystallites in the powders, obtained by the hydrothermal method and the Pechini method, amounted to respectively about 14 and 24 nm.

The BET specific surface area determined from the nitrogen adsorption measurements amounted to 102 and $22 \text{ m}^2\text{g}^{-1}$ for the $\text{CaKCe}(\text{PO}_4)_2$ powders obtained by respectively the hydrothermal method and the Pechini method. The average size of the grains in the obtained samples was calculated on the basis of the determined specific surface area of the powders. The average grain size amounts to 16 nm for the hydrothermally obtained phosphate and

75 nm for the powder synthesized by the Pechini method. The difference in the determined grain and crystallite sizes of the powders obtained by the Pechini method may indicate the presence of aggregates made up of several crystallites. This was confirmed by TEM imaging of powders. Fig. 3 presents TEM and HRTEM images of samples obtained by hydrothermal and Pechini techniques. The powder synthesized by Pechini method is characterized by presence of aggregates with nanocrystals with diameter up to 30 nm (Fig. 3A and B). The TEM images of sample obtained under hydrothermal conditions revealed the sample to be built of round shaped nanocrystals with the diameter of about 15 nm (Fig. 3C and D).

The sample obtained by ceramic method was characterized by much lower BET specific surface. Moreover, grinding (for 5 min at 40 Hz) in a vibrating mill of the sample resulted in increase of specific surface area value from $0.05 \text{ m}^2\text{g}^{-1}$ to $0.687 \text{ m}^2\text{g}^{-1}$. The very effective grinding is connected with a reduction in grain size from 33 to $2.4 \mu\text{m}$.

The DTA/DSC analyses of the samples showed that $\text{CaKCe}(\text{PO}_4)_2$ doesn't undergo any polymorphic change since no thermal effects appeared on the curves. However, in a temperature range of 1300–1400 °C a small mass loss of the compound (up to about 2 wt.%) was observed. The TGA curves of samples obtained by different methods are shown in Fig. 4.

The existence of the polymorphic change of compound $\text{CaKLa}(\text{PO}_4)_2$ at 1120 °C was postulated in [11], where the phosphate was obtained from LaPO_4 (monazite) and CaKPO_4 using the ceramic method and long-term sintering at 1200 °C. At the same time the research by Campayo et al. [3,14] showed that the yield of $\text{MeMLn}(\text{PO}_4)_2$ (Me : Ca, Sr; M : Cs, K) compounds by the synthesis in solid state does not exceed 78%. The low yield of the reaction is due to two facts. First of all, monazites are compounds characterized by very low reactivity against alkalis and acids and by stability at high temperatures [32–34]. Moreover, during sintering of substrates at a temperature of 1200 °C the $\text{MeMNd}(\text{PO}_4)_2$ phosphates are depleted of potassium/caesium and phosphorous, whereby a secondary phase, i.e. $\text{Ca}_3(\text{PO}_4)_2$, forms. This calcium orthophosphate undergoes a polymorphic transition at about 1120 °C [35,36]. The same transition temperature was reported by Jungowska for the $\text{CaKLa}(\text{PO}_4)_2$ compound [11]. This means that the thermal effects observed on the DTA/DSC curves in [11] may have been connected with the polymorphic transition $\beta \rightarrow \alpha\text{-Ca}_3(\text{PO}_4)_2$. From experimental results presented in this study and other literature reports [3,14] it appears that the $\text{CaKLn}(\text{PO}_4)_2$ phase has only one structural form and the thermal effects in the DTA curves observed in [11] could have been connected with the presence of $\text{Ca}_3(\text{PO}_4)_2$ due to the inhomogeneity of the samples or to the partial decomposition of the $\text{CaKLa}(\text{PO}_4)_2$ phosphate.

The decrement in the mass of the $\text{CaKCe}(\text{PO}_4)_2$ compound registered at the TGA curves of the compound was attributed to the partial decomposition of this phase as a result of an incongruent sublimation of more volatile components, i.e. probably gaseous phosphorous and potassium species. The sublimation process changes the chemical composition of the solid phase, causing the decomposition of $\text{CaKCe}(\text{PO}_4)_2$. Similar remarks considering the limited stability of $\text{MMeNd}(\text{PO}_4)_2$ phases as a result of depletion of Cs/K and phosphorous in the course of high temperature treatment were reported in previously published papers [3,14].

In order to determine the thermal stability of $\text{CaKCe}(\text{PO}_4)_2$ the powders obtained by the hydrothermal and the ceramic methods were additionally annealed at a temperature of 1200 °C for 120 h. The main change in the phase composition of the preparations was found in the hydrothermally synthesized sample. The X-ray diffraction patterns of the sample sintered at different temperatures are shown in Fig. 5. An analysis of the diffractograms showed that $\text{CaKCe}(\text{PO}_4)_2$ had undergone complete decomposition into

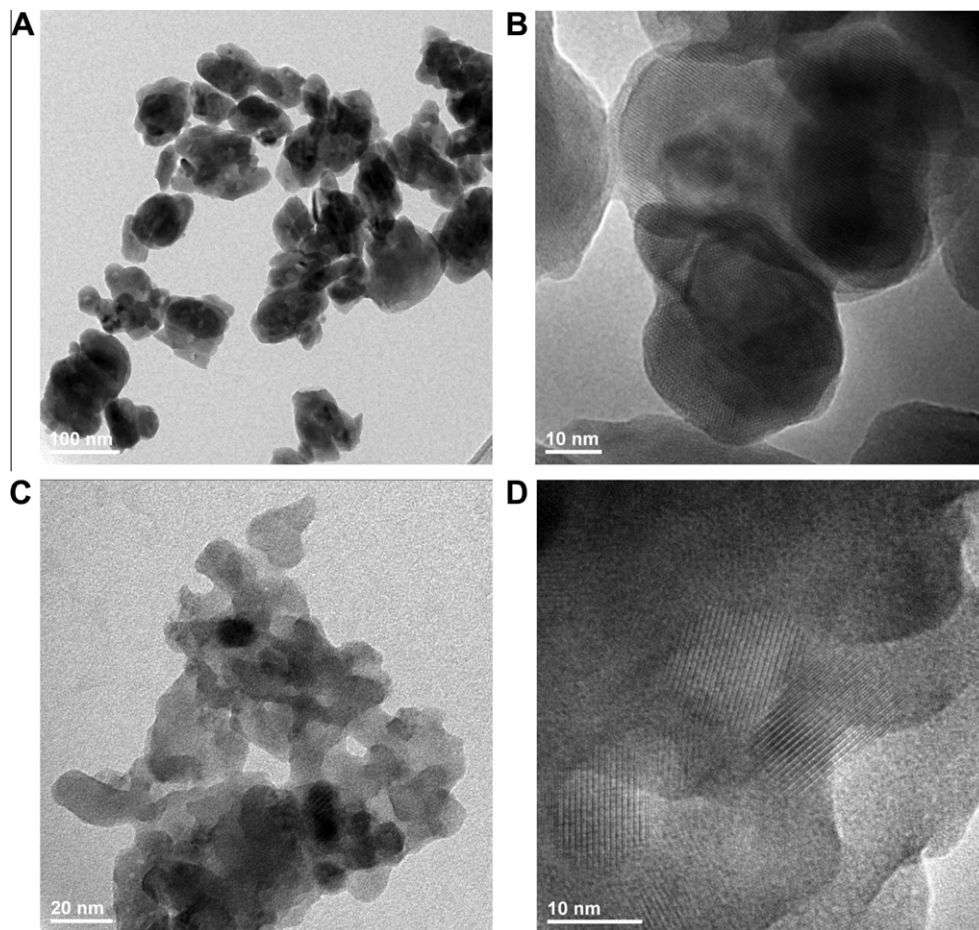


Fig. 3. The TEM and HRTEM images of samples obtained by Pechini (A and B) and hydrothermal methods (C and D).

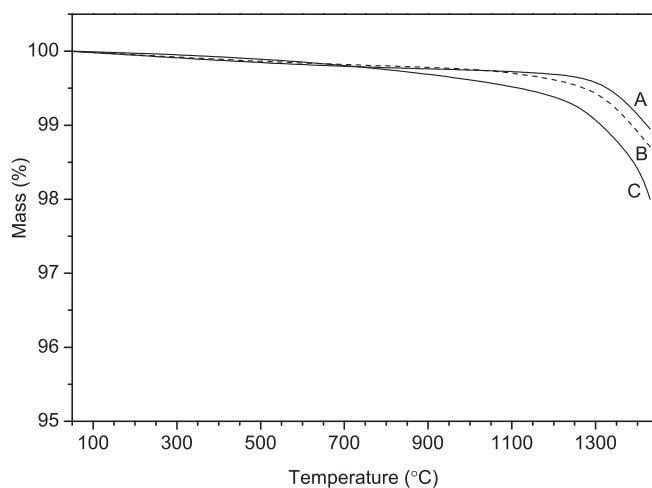


Fig. 4. The TGA curves of $\text{CaKCe}(\text{PO}_4)_2$ compound obtained by Pechini method (A), in solid state (B) and in hydrothermal process (C). Experiments carried out in air atmosphere.

phases: $\text{Ca}_{10}\text{K}(\text{PO}_4)_7$, CeO_2 and CePO_4 in the course of long-term annealing at 1200°C . In the sample synthesized by the ceramic method and sintered at elevated temperature no secondary phases were found to be present. Thus the presence of the secondary phases in the powders could have been below the detection limit of the XRD technique.

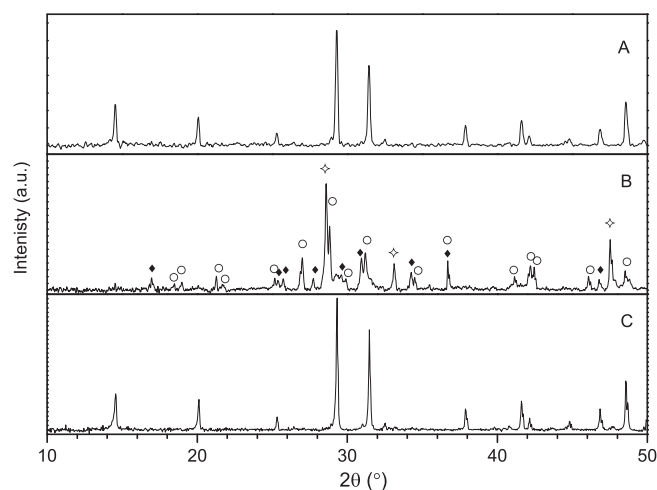
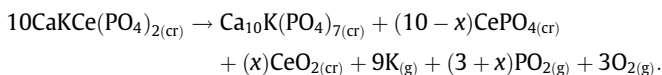


Fig. 5. The XRD patterns of $\text{CaKCe}(\text{PO}_4)_2$ compound synthesized by the hydrothermal method after sintering 1 h at 1000°C (A) and 120 h at 1200°C (B), as well as the sample obtained by ceramic method heated 120 h at 1200°C (C). [\circ – CePO_4 (monazite), \diamond – CeO_2 , \blacklozenge – $\text{Ca}_{10}\text{K}(\text{PO}_4)_7$].

Unfortunately, the chemical analysis of the sample which had undergone thermal decomposition was not possible because of the low reactivity of the formed phases. The solid residues could not be digested even in aqua regia. However, the analysis of the results obtained by the XRD method allows to conclude as follows:

- at elevated temperature $\text{CaKCe}(\text{PO}_4)_2$ undergoes decomposition into $\text{Ca}_{10}\text{K}(\text{PO}_4)_7$, CeO_2 and CePO_4 .
- from the elemental balance and the data on the sublimation of orthophosphates [37] the following decomposition route of ternary phosphate could be proposed:



The scheme indicates considerable change in the phase composition of ternary phosphate in the course of sintering. This is a result of sublimation of potassium and phosphorous species from solid phase. At the same time it should be noted that the chemical composition of compound $\text{Ca}_{10}\text{K}(\text{PO}_4)_7$ corresponds to a concentration range in which a solid solution of CaKPO_4 in $\beta\text{-Ca}_3(\text{PO}_4)_2$ exists [16]. In addition $\text{Ca}_{10}\text{K}(\text{PO}_4)_7$ is isostructural with the low-temperature $\text{Ca}_3(\text{PO}_4)_2$ form [38]. This means that it is difficult to distinguish compounds $\text{Ca}_{10}\text{K}(\text{PO}_4)_7$ and $\beta\text{-Ca}_3(\text{PO}_4)_2$ on the basis of XRD spectra, and $\beta\text{-Ca}_3(\text{PO}_4)_2$ instead of $\text{Ca}_{10}\text{K}(\text{PO}_4)_7$ may be actually observed in the sample after sintering. Thus the decomposition of $\text{CaKCe}(\text{PO}_4)_2$ phase may proceed gradually until potassium completely evaporates from the sample and $\beta\text{-Ca}_3(\text{PO}_4)_2$ forms. The proposed decomposition scheme is also in accordance with previously mentioned studies of thermal stability of ternary phosphates [3,14].

The observed differences in the intensity of the decomposition of the ternary phosphate obtained by the ceramic method and the hydrothermal method can be explained by the different specific surface areas of the samples (102 and $0.05 \text{ m}^2\text{g}^{-1}$ respectively for powders obtained by hydrothermal and ceramic method), since the sublimation processes largely depend on the size and quality of the material surface.

3.2. Phase equilibria in the $\text{CaKPO}_4\text{-CePO}_4$ system

Because of the limited thermal stability of compounds present in the system, it was necessary to reduce the temperature and sintering time of samples used in the phase equilibrium study. Consequently, the samples were several times pelletized and ground between heating steps. Owing to this the phase equilibrium in the samples could be reached easier.

An analysis of the X-ray spectra of the samples sintered from the $\text{CaKPO}_4\text{-CePO}_4$ system showed all the samples, except for CaKPO_4 , $\text{CaKCe}(\text{PO}_4)_2$ and CePO_4 compounds, to be diphasic. In the samples containing less than 50 mol.% of CePO_4 , CaKPO_4 and $\text{CaKCe}(\text{PO}_4)_2$ phases were found to coexist.

The DSC results confirmed the presence of phase CaKPO_4 in the samples. Fig. 6 shows the DSC curves for the heating of the samples selected from the $\text{CaKPO}_4\text{-CaKCe}(\text{PO}_4)_2$ phase area. In the temperature range of $600\text{--}700^\circ\text{C}$, two endothermic effects were observed on the heating curves. Both effects are connected with the polymorphic transition of CaKPO_4 [16]. As the molar fraction of CePO_4 increased, the intensity of the effects decreased, but the change of chemical composition of samples had no influence on the onset temperatures of effects. Since the temperatures were constant and independent of the $\text{CaKCe}(\text{PO}_4)_2$ content in the samples, the formation of any solid solution within the composition range of $\text{CaKPO}_4\text{-CaKCe}(\text{PO}_4)_2$ could be ruled out.

The samples with more than 50 mol.% of CePO_4 were also diphasic. The diffraction spectra of the synthesized powders showed compounds $\text{CaKCe}(\text{PO}_4)_2$ and CePO_4 to be present in them. The DTA-heating curves for the samples did not show any thermal effects in the temperature range of $20\text{--}1400^\circ\text{C}$.

All the registered onset temperatures of thermal effects reflected on the heating DTA/DSC curves of samples in the $\text{CaKPO}_4\text{-}$

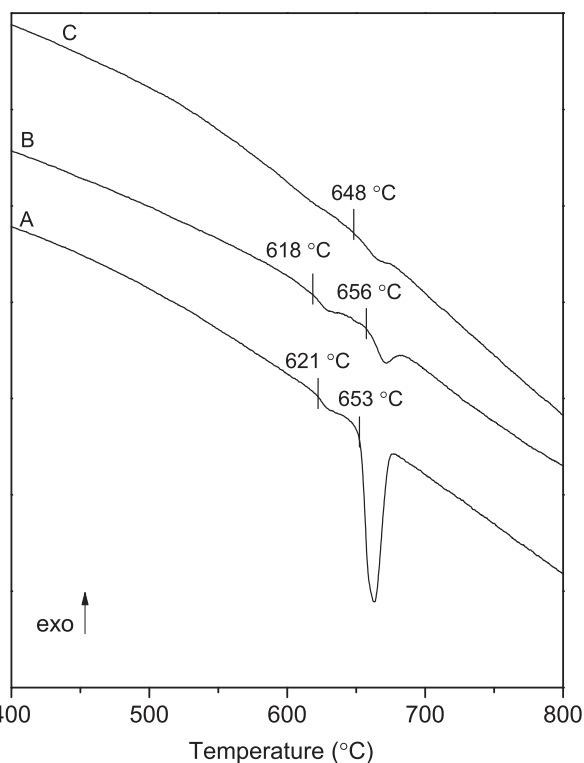


Fig. 6. The DSC heating curves of samples with $x(\text{CePO}_4) = 0$ (A), 0.25 (B) and 0.45 (C).

CePO_4 system are shown in Fig. 7. The same figure summarizes also samples melting points, determined by the experiments in horizontal furnaces. Due to very high temperatures of experiments and limited equipment stability it was not possible to determine melting temperatures of samples with $x(\text{CePO}_4) > 0.75$. The phase composition of samples ground after melting experiments was examined by XRD and microscopic observations of polished cross sections of samples cooled from melt. The XRD results did not show presence of phases other than $\text{CaKCe}(\text{PO}_4)_2$, CaKPO_4 or CePO_4 . Nevertheless, because of the limited thermal stability of the phases present in the system, the presented in the Fig. 7 liquidus shape in the area rich in CePO_4 is as proposed.

The chemical composition of an eutectic point and its temperature were determined from the distribution of samples melting temperatures. Fig. 8 shows microphotographs of cross sections of samples with $x(\text{CePO}_4) = 0.25$ and 0.50 . The microstructure of the sample with $x(\text{CePO}_4) = 0.25$ (Fig. 8A) is characteristic of an eutectic point. Whereas in the cross section of the sample with $x = 0.50$, i.e. compound $\text{CaKCe}(\text{PO}_4)_2$, large polyhedral grains of about $30 \times 100 \mu\text{m}$ in size are visible (Fig. 8B). The grains were visible in all samples with $0.25 < x(\text{CePO}_4) < 0.60$. Small acicular and light in color inclusions can be distinguished within the polyhedral grains. The amount of the segregations increased with CePO_4 content. Analysis of XRD patterns of the $\text{CaKCe}(\text{PO}_4)_2$ compound after crystallization from melt showed that the sample was diphasic. Besides ternary phosphate a small amount of CePO_4 was found to be present. The appearance of the latter phase in the sample can be indicative of the partial decomposition of $\text{CaKCe}(\text{PO}_4)_2$ at temperatures above 1200°C , as already discussed above. However, considering that no $\text{Ca}_3(\text{PO}_4)_2$, in any of its polymorphic forms, was found to be present in the sample, another probable explanation of CePO_4 presence is possible. The distribution of the melting temperatures of samples with 45–75 mol.% CePO_4 content does not show any maximum. This kind of temperatures distribution is

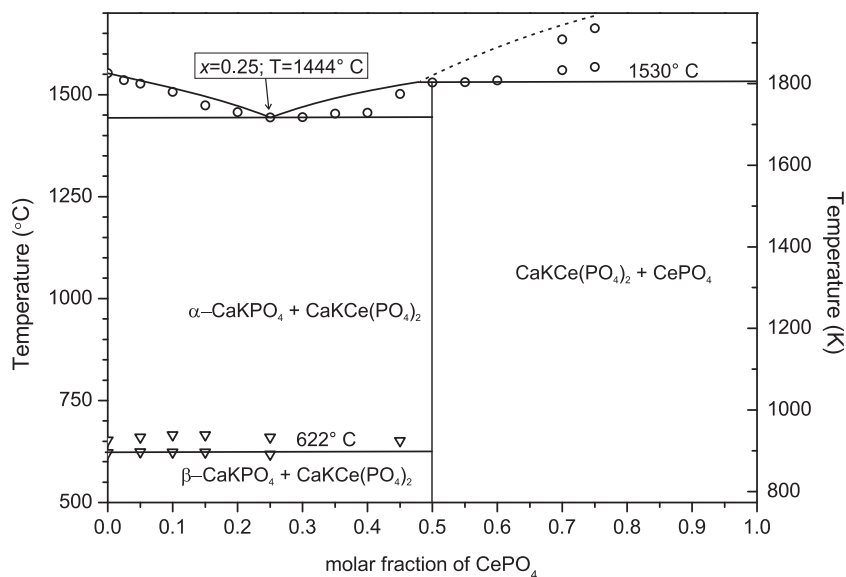


Fig. 7. Phase diagram of $\text{CaKPO}_4\text{-CePO}_4$ system. [∇ – onset temperatures of endothermic effects registered on DTA/DSC heating curves, \circ – melting temperatures of samples determined by optical observation of pellets].

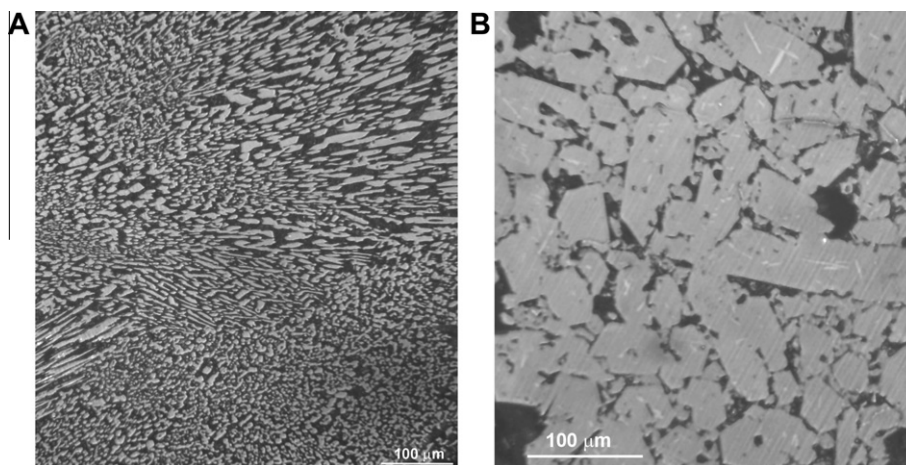
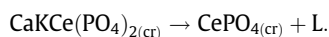


Fig. 8. The microstructure of samples cooled from melt with $x(\text{CePO}_4) = 0.25$ (A) and 0.50 (B).

indicative of peritectic reaction of compound $\text{CaKCe}(\text{PO}_4)_2$, proceeding according to the scheme:



During crystallization of sample with $x(\text{CePO}_4) = 0.50$ from temperatures higher than the temperature of the peritectic reaction, monazite (CePO_4) crystallizes first and only when $T \leq T_{\text{per}}$ the latter compound starts reacting with liquid being in equilibrium, forming $\text{CaKCe}(\text{PO}_4)_2$. The crystallization of ternary phosphate takes place at liquid/monazite interface. Thus if the sample is cooled down from the high temperatures too quickly (in non-equilibrium conditions) the crystallization of $\text{CaKCe}(\text{PO}_4)_2$ may be incomplete. As a result, unreacted CePO_4 may be present inside the grains of the ternary phosphate. This should be accompanied by the appearance of vitrified liquid phase in the cooled samples. This microstructure of compound $\text{CaKCe}(\text{PO}_4)_2$ is visible in Fig. 8B. Thus the presence of the secondary crystalline phase (CePO_4) may be due to the non-equilibrium state of the sample, caused by the too rapid cooling from melt.

4. Conclusions

The results of the study provided the basis for proposing a diagram representing the phase equilibria in the $\text{CaKPO}_4\text{-CePO}_4$ system (Fig. 7). Compound $\text{CaKCe}(\text{PO}_4)_2$ forms in the $\text{CaKPO}_4\text{-CePO}_4$ system and an eutectic point was found to be present at $T = 1444^\circ\text{C}$ for $x(\text{CePO}_4) = 0.25$. The results of XRD and thermal analysis experiments did not show any solid solution to be present in the system examined.

Compound $\text{CaKCe}(\text{PO}_4)_2$ has a hexagonal structure of the rhabdophane type, with unit-cell parameters $a = b = 7.0468(8) \text{ \AA}$ and $c = 6.4367(0) \text{ \AA}$. The compound does not undergo any polymorphic transitions. It is characterized by limited thermal stability at temperatures above 1200°C , however rate of the decomposition of the phosphate depends on the specific surface area value of powder. Compound $\text{CaKCe}(\text{PO}_4)_2$ melts incongruently at a temperature of 1530°C .

According to the previously published studies on the subject, the ceramic method's yield of phase-pure $\text{MMeLn}(\text{PO}_4)_2$ samples is limited. In this study, in order to improve the yield of $\text{CaKCe}(\text{PO}_4)_2$, the solid-phase syntheses were conducted in stages,

whereby the sintering of samples at temperatures below 1100 °C was preferred. Efficient grinding of samples in vibrating ball mill and pelletizing of the samples were employed too to enhance reactivity of substrates. As a result, homogenous samples and phase pure CaKCe(PO₄)₂ phosphate were obtained. In addition, two alternative methods of CaKCe(PO₄)₂ synthesis (hydrothermal and Pechini modified techniques) have been developed. Both of them enable obtaining of the compound at low temperatures (up to 500 °C) and with nanometric crystallite size.

Acknowledgements

The study was financially supported by Polish Ministry of Science and Higher Education under grant JP 2010 024870 and by National Science Centre under grant N N209 767240. The authors acknowledge Prof. L. Kępiński for the possibility and help with TEM measurements.

References

- [1] C. Parent, P. Bochu, G. Le Flem, P. Hagenmuller, J.C. Bourcet, F. Gaume-Mahn, J. Phys. Chem. Solids 45 (1984) 39–45.
- [2] S. Tie, Q. Su, Y. Yu, Phys. Stat. Sol. A 147 (1995) 267–276.
- [3] L. Campayo, F. Audubert, J.-E. Lartigue, S. Botuha, D. Bernache-Assolant, J. Nuclear Mater. 374 (2008) 101–108.
- [4] A.M. Band, S.J. Dhoble, R.B. Pode, Bull. Mater. Sci. 22 (1999) 965–969.
- [5] Z.J. Zhang, J.L. Yuan, S. Chen, H.H. Chen, X.X. Yang, J.T. Zhao, G.B. Zhang, C.S. Shi, Opt. Mater. 30 (2008) 1848–1853.
- [6] C. Parent, P. Bochu, A. Daoudi, G. Le Flem, J. Solid State Chem. 43 (1982) 190–195.
- [7] D. Wang, Y. Wang, Mater. Sci. Eng. B 133 (2006) 218–221.
- [8] Z.J. Zhang, J.L. Yuan, C.J. Duan, D.B. Xiong, H.H. Chen, J.T. Zhao, G.B. Zhang, C.S. Shi, J. Appl. Phys. 102 (2007) 093514.
- [9] Z.J. Zhang, S. Chen, J. Wang, H.H. Chen, X.X. Yang, J.T. Zhao, Y. Tao, Y. Huang, Opt. Mater. 32 (2009) 99–103.
- [10] Y.C. Chen, W.Y. Huang, T.M. Chen, J. Rare Earths 29 (2011) 907–910.
- [11] W. Jungowska, Solid State Sci. 9 (2007) 318–321.
- [12] M. Vlasse, P. Bochu, C. Parent, J.P. Cheminade, A. Daoudi, G. Le Flem, P. Hagenmuller, Acta Cryst. B 38 (1982) 2328–2331.
- [13] A. Arbus, C. Duranceu, D. Zambon, J.C. Cousseins, Eur. J. Solid State Inorg. Chem. 28 (1991) 499–502.
- [14] L. Campayo, F. Audubert, D. Bernache-Assolant, Solid State Ionics 176 (2005) 2663–2669.
- [15] M.A. Bredig, J. Phys. Chem. 46 (1942) 747–764.
- [16] T. Znamierowska, Zeszyty Naukowe Politechniki Slaskiej 709 (1982) 15–21.
- [17] G.W. Beall, L.A. Boatner, D.F. Mullica, W.O. Milligan, J. Inorg. Nucl. Chem. 43 (1981) 101–105.
- [18] J.G. Pepin, E.R. Vance, J. Inorg. Nucl. Chem. 43 (1981) 2807–2809.
- [19] Y. Hikichi, T. Nomura, J. Am. Ceram. Soc. 70 (1987) C252–C253.
- [20] L. Macalik, P.E. Tomaszewski, A. Matraszek, I. Szczygieł, P. Solarz, P. Godlewska, M. Sobczyk, J. Hanuza, J. Alloys Compd. 509 (2011) 7458–7465.
- [21] M.P. Pechini, US Patent 3330697, July 11, 1967.
- [22] A. Matraszek, E. Radomińska, I. Szczygieł, J. Therm. Anal. Calorim. 103 (2011) 813–819.
- [23] D. Mizer, L. Macalik, P.E. Tomaszewski, R. Lisiecki, P. Godlewska, A. Matraszek, I. Szczygieł, M. Zawadzki, J. Hanuza, J. Nansci. Nanotechnol. 9 (2009) 5164–5169.
- [24] W. Jungowska, Solid State Sci. 4 (2002) 229–232.
- [25] A. Matraszek, I. Szczygieł, J. Am. Ceram. Soc. 95 (2012) 3651–3656.
- [26] W. Szuszkiewicz, E. Radomińska, T. Znamierowska, P. Wilk, Pol. J. Chem. 76 (2002) 1095–1100.
- [27] B.I. Lazoryak, V.N. Golubev, R. Salmon, C. Parent, P. Hagenmuller, Eur. J. Solid State Inorg. Chem. 26 (1989) 455–463.
- [28] J. Laugier, B. Bochu, LMGP-Suite of Programs for the Interpretation of X-ray Experiments, ENSP Laboratoire des Materiaux et du Genie Physique, BP, Saint Martin d'Herès, France, 2004.
- [29] R.D. Shannon, Acta Cryst. A 32 (1972) 751–767.
- [30] S. Tie, Q. Su, Y. Yu, J. Alloys Compd. 227 (1995) 1–4.
- [31] H.P. Klug, L.E. Alexander, X-ray Diffraction Procedures for Polycrystalline and Amorphous Materials, Wiley & Sons, New York, 1974.
- [32] N. Clavier, N. Dacheux, Inorg. Chem. 45 (2006) 220–229.
- [33] R. Podor, M. Cuney, C.N. Trung, Am. Miner. 80 (1995) 1261–1268.
- [34] D.B. Kitaev, Y.F. Volkov, A.I. Orlova, Radiochemistry 46 (2004) 211–217.
- [35] J.H. Welch, W. Gutt, J. Chem. Soc. (1961) 4442–4444.
- [36] I. Barin, Thermochemical Data of Pure Substances, Part I-II., VCH Verlags Gesellschaft, Weinheim, Germany, 1993.
- [37] V.L. Stolyarova, G.A. Semenov, in: J.H. Beynon (Ed.), Mass Spectrometric Study of the Vaporization of Oxide Systems, Wiley, New York, 1994.
- [38] PC PDF Win v. 1.30, Inorganic Compounds, International Centre for Diffraction Data (ASTM), 1997.